Project 050 Over-Wing Engine Placement Evaluation

Georgia Institute of Technology

Project Lead Investigator

Principal Investigator
Professor Dimitri N. Mavris
Director, Aerospace Systems Design Laboratory
School of Aerospace Engineering
Georgia Institute of Technology
Phone: (404) 894-1557
Fax: (404) 894-6596
Email: dimitri.mavris@ae.gatech.edu

Co-Principal Investigator
Dr. Chung Lee
Research Engineer
Aerospace Systems Design Laboratory
School of Aerospace Engineering
Georgia Institute of Technology
Phone: (404) 894-0197
Fax: (404) 894-6596
Email: chung.h.lee@ae.gatech.edu

University Participants

Georgia Institute of Technology

- PI: Dr. Dimitri Mavris; Co-PI: Dr. Chung Lee
- FAA Award Number: 13-C-AJFE-GIT-057
- Period of Performance: February 5, 2020 to June 4, 2022
- Tasks relevant for this period:
  1. Architecting design strategy
  2. Select aero-propulsion integration method
  3. Create aircraft mission and engine models
  4. Reduce dimensionality using active subspace methods
  5. Perform computational fluid dynamics (CFD) grid sensitivity analysis
  6. Complete first stage design study (nacelle location selection)
  7. Create Aircraft Noise Prediction Program (ANOPP) noise surrogate models

Project Funding Level

The Georgia Institute of Technology (Georgia Tech) was funded at $590,000 for a two-year project and has agreed to a total of $590,000 in matching funds. This total includes salaries for the project director, research engineers, and graduate research assistants, as well as computational, financial, and administrative support, including meeting arrangements. The institute has also agreed to provide tuition remission for the students, paid for by state funds.

Investigation Team

PI: Dimitri Mavris
Co-Investigator: Chung Lee
Aerodynamics and parametric geometry: Jai Ahuja, Srujal Patel, Kenneth Decker
Multidisciplinary Design Analysis and Optimization (MDAO) methods: Christian Perron
Mission and systems integration: Evan Harrison

Graduate students: Mengzhen Chen, Sam Crawford, Marc Koerschner, Bilal Mufti, James Van der Linden, Anish Vegesna

Project Overview

The over-wing nacelle (OWN) aircraft concept has promising environmental benefits due to shielding of engine noise by the wings and the potential to reduce landing gear height and therefore gear noise. However, if not optimized, engine placement in OWN aircraft may cause penalties in fuel burn due to aerodynamic interactions between the wing and propulsor. Our project involves developing a multidisciplinary analysis and optimization (MDAO) method for OWN aircraft. This task builds on past efforts by including noise shielding effects and analyzing multiple flight conditions to minimize fuel burn. One major challenge in this project is the computational expense of analyses such as CFD. Our approach relies on MDAO and efficient adaptive sampling techniques to use high fidelity analyses only where they are most needed for system analysis.

The optimization of an OWN aircraft configuration over a mission with noise constraints will enable accurate assessments of the tradeoffs between noise benefits and fuel burn. As a secondary benefit, the MDAO method will demonstrate efficient sampling methods for coupled, computationally intensive simulations in system analysis. These methods are useful to the FAA because many current applications require high-fidelity simulations to accurately assess physical phenomena such as noise and emissions. Both the OWN results and the MDAO techniques used here will enable more physics-informed decisions about the environment.

The 2020 work focused on preliminary tasks to prepare a software tool chain and workflow for optimization, and in 2021, it focused on executing a full-scale MDAO process using supercomputing resources. The 2021 project thus focused on a two-stage design process: nacelle location selection followed by preliminary shape optimization of the wing and nacelle. Over the first six months of 2022, we will finish the optimization analysis, integrate aero-propulsion with mission and systems, and conduct supporting studies of detailed design sensitivities and scenarios.

We emphasized two major themes in our 2021 research methodology: 1) a more controlled comparison of OWN vs. under-wing nacelle (UWN) and 2) careful accounting for numerical uncertainty.

A more controlled comparison of OWN and UWN

Uncertainty in the physics code dominated the MDAO and research strategies. There can be significant discrepancies between un-calibrated CFD predictions and the flight performance of actual vehicles. Therefore, in the absence of validation data, it would be uninformative or misleading to compare the CFD-based performance of an optimized OWN vehicle with that of actual UWN vehicles. In addition to the physics discrepancy, there is an inconsistency in that the MDAO problem for OWN has only been studied for two years, whereas the UWN configuration has been refined by the aircraft industry for around seventy years!

The present OWN study cannot practically include additional aspects of design physics such as flight mechanics, static and dynamic structural constraints, nacelle geometry constraints due to acoustical liners and de-icing components, and pylon aero-thermo-structural mechanics. However, this can result in OWN performance that is overly optimistic due to an under-constrained problem formulation. It can lead to unrealistic conclusions about OWN compared to traditional UWN.

The goal is to provide FAA stakeholders with evidence to assess the intrinsic aero-propulsive advantages and disadvantages of OWN and UWN aircraft. It is impossible to pose a perfectly controlled experiment. However, we adopted a “drag race” approach in which we optimized OWN and UWN vehicles under the same MDAO formulation. This is an important decision in study methodology: it halves the computational budget available to optimize each configuration but leads to a more controlled comparison and more credible conclusions.

Uncertainty is a key theme

During our 2021 research, we found that careful quantification of uncertainty is crucial to avoiding misleading or less credible conclusions about the benefits of OWN. There are no relevant empirical data for the direct validation or calibration of OWN or even UWN with powered turbofan engines. However, even controlling the numerical uncertainties due to CFD or MDA is important. We have incorporated such uncertainty tracking into the optimization strategy itself. For example, we avoid optimization or adaptive sampling below an “uncertainty floor” of the physics code.

We found that much of the recent published literature on OWN relied on CFD meshes on the order of 0.8 to 30 million cells or nodes. Different CFD meshes and solvers have different dependences between mesh density and solution accuracy. For

example, solvers may be either node-centered or cell-centered, and different solvers will have different orders of formal accuracy due to their different computational stencils. Variation in user skill can also lead to different accuracy given similar cell counts. Nonetheless, most previous academic and industry studies have not included mesh sensitivity studies or accounted for the numerical uncertainty due to the mesh. This of critical importance. For example, there is a risk of reporting a "-1% Δfuel burn benefit of OWN vs. UWN," even though the uncertainty is much greater than 1%.

Careful attention to valid OWN vs UWN comparison and numerical uncertainty thus informed much of the detailed work in our 2021 tasks. We believe that such a research strategy prevents us from making a simplistic performance comparison between the two configurations and will instead yield more credible and complex conclusions that can inform FAA stakeholders about the potential environmental impacts of each configuration.

Details of 2021 tasks are described in following sections.

Notation and Abbreviations

α: angle of attack
ANN: artificial neural network
C_D: drag coefficient
C_L: lift coefficient
CFD: computational fluid dynamics
CRM: NASA Common Research Model
η_{pr}: inlet pressure recovery
MDAO: multidisciplinary design analysis and optimization
OWN: over-wing nacelle
p_{s2}: static pressure at inlet
p_{t8}: total pressure at core nozzle exit
p_{t18}: total pressure at bypass nozzle exit
T_{t8}: total temperature at core nozzle exit
T_{t18}: total temperature at bypass nozzle exit
UWN: under-wing nacelle
O( ): order of magnitude

Task 1 - Architecting of Design Process

Georgia Institute of Technology

Objective(s)

The overall goal is to design a problem architecture for multidisciplinary analysis and optimization (MDAO) to assess a single-aisle OWN transport aircraft. The MDAO process will use CFD, noise analysis codes such as ANOPP, as well as weights, engine cycle, and mission analysis. The formulation was stated in the first year of the project and has evolved during the project due to physics results. However, the working MDAO problem statement was adopted:

- **Minimize** fuel burn for a baseline mission
- **Subject to** design variables including aircraft range, takeoff field length, and detailed side constraints
- **With respect to** design variables including engine nacelle position (focusing on forward placement), nacelle and wing geometry, engine cycle, and operating condition
- **Given** a baseline single-aisle aircraft model and mission profile
- **Returning** fuel burn and noise

In discussion with FAA technical advisors, it was decided to place more emphasis on aerodynamic performance optimization rather than noise reduction, which is necessarily of lower fidelity. Thus, the single objective function in our MDAO problem statement is minimizing fuel burn, but noise is still evaluated as a response with respect to design variables. It is anticipated that the MDAO problem will undergo several iterations as more information accumulates, so noise may be later treated as a constraint or secondary objective.

Research Approach

Aerodynamics is the most computationally expensive physics discipline, coupled closely with propulsion cycle analysis. Therefore, the 2021 efforts were focused on the most important aero-propulsion aspects of MDAO, which drive the overall architecture of the problem.

Preliminary aero-propulsion subset of the MDAO problem:

Minimize	fuel burn
With respect to	geometry, angle of attack α, and engine mass flow
Given	fixed engine cycle design and throttle assumptions; no pylon
Subject to	continuity (mass flow balance between inlet and outlet)
	momentum balance (e.g., lift = weight, thrust = drag in steady level flight)
	interdisciplinary consistency:
	inlet pressure recovery $p_{t2,CFD} = p_{t2,cycle\ analysis}$
	core nozzle total pressure $p_{t8,CFD} = p_{t8,cycle\ analysis}$
	core nozzle total temperature $T_{t8,CFD} = T_{t8,cycle\ analysis}$
	bypass nozzle total pressure $p_{t18,CFD} = p_{t18,cycle\ analysis}$
	bypass nozzle total temperature $T_{t18,CFD} = T_{t18,cycle\ analysis}$
Returning	fuel burn

Two-Stage Design Strategy

The geometry design variables included 45 shape parameters for the nacelle and wing, which were reduced to smaller dimensions in a task described later in this report. Due to the curse of dimensionality (or the rapid increase in computational expense with increased dimensionality), the MDAO process was staged into two distinct steps:

- Stage 1: Commit to a nacelle location based on an "open-loop" aero-propulsion parametric optimization
- Stage 2: Perform MDAO of nacelle and wing shape given the fixed nacelle location

Stage 1 Strategy

Stage 1 assumed a fixed Y (spanwise) location for the nacelle because that location is typically optimized using structural analysis. The nacelle location plays a major role in relieving both static and dynamic loads on the wing. The baseline geometry for this study is the NASA Common Research Model (CRM) scaled to a typical 150-pax size [Vassberg et al, 2008]. Because structural analysis is beyond the scope of the project, we conservatively defaulted the spanwise location to that of the scaled CRM.

Stage 1 used a parametric optimization approach. We defined f as an objective function of parameter or scenario variables and "choice" variables:

$$f = f(\underline{\mathbf{X}}_{parameter}, \underline{\mathbf{X}}_{choice})$$

In this case, $\underline{\mathbf{X}}_{parameter}$ are the nacelle locations ($x_{nacelle}$, $y_{nacelle}$) following the coordinate directions in Figure 1. $\underline{\mathbf{X}}_{choice}$ are more detailed shape variables. The goal of parametric optimization is to minimize f with respect to $\underline{\mathbf{X}}_{choice}$ for any instance of $\underline{\mathbf{X}}_{parameter}$. In other words, we aimed to provide a map of aero-propulsive performance over locations ($x_{nacelle}$, $y_{nacelle}$) while sufficiently optimizing the shape at each location. The intent was to "give a fair shake" to potential nacelle locations by conducting

balanced optimization for each. The cartoon in Figure 2 shows notionally that there is a grid or DoE of settings for $\underline{\mathbf{X}}_{parameter}$. For each instance of $\underline{\mathbf{X}}_{parameter}$, there is a search in the direction of $\underline{\mathbf{X}}_{choice}$ to find the particular optimum.

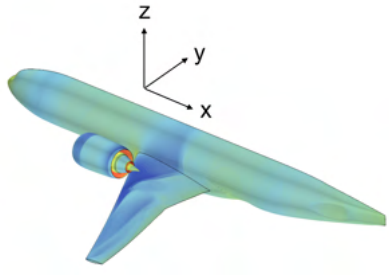

Figure 1. Coordinate system.

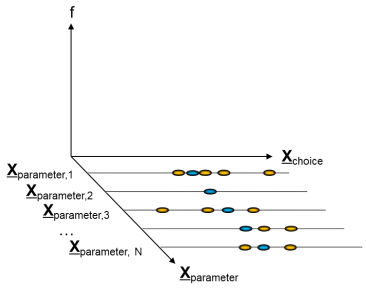

Figure 2. Cartoon representation of parametric optimization
(Adaptive sampling typically began with a "warm-start" of blue seed points).

An equally weighted sum of the lift-to-drag ratio (L/D) and the excess thrust (normalized to a reference case) was used as the objective function *f*. To limit the number of analysis iterations, this initial study used open-loop aero-propulsion MDA. Iterative looping (Gauss-Seidel) or similar procedures were not used to tightly enforce interdisciplinary consistency between a propulsion cycle analysis and CFD aerodynamics.

The Stage 1 parametric optimization was performed with a Bayesian adaptive sampling technique. This approach sequentially fit a Gaussian Process or kriging model and added new sample points according to an acquisition function or infill criterion. In our case, we used the expected improvement (EI) infill criterion. EI has been described by previous literature such as Jones, Schonlau, and Welch (1998) and is shown notionally in Figure 3 below.

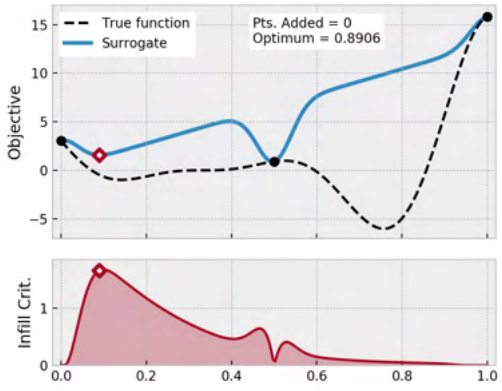

Figure 3. Snapshot of an adaptive sampling process. The infill criterion is maximized to identify the most favorable location for evaluating a sample point.

A grid of x-z nacelle locations was sampled, and propulsion/CFD analyses were sequentially run at design points that maximized the expected improvement within each particular x-z location. This procedure was carried out until the EI was of a similar order of magnitude as the numerical uncertainty due to the CFD grid (described in a later section).

Earlier in this period of performance, we were aware of a major risk of this Stage 1 parametric optimization: that it may not reveal a truly optimal location for the over-wing nacelle. We discussed with our FAA technical advisors that this outcome is both possible and likely due to an under-constrained MDAO problem. A full MDAO problem would include the physics of many other disciplines, including structural weight penalties and trim drag due to pitching moments. In our limited project scope, we focused on static aerodynamics and propulsion analyses, so we might find that L/D and excess thrust simply improve monotonically as the nacelle moves farther up and forward (i.e., farther from the influence of the wing). Indeed, this is the result discussed under a later task.

Because this ambivalent outcome for Stage 1, we discussed with FAA advisors that we would quantify a map of performance over nacelle x-z locations but may then simply select a new reference location for further optimization in Stage 2. This was indeed the outcome of Stage 1.

Stage 2 Strategy

After selecting a new reference location for the OWN, the number of design variables was expanded. Rather than repeat the parametric optimization used in Stage 1, this larger-scale MDAO uses a simple optimization formulation. As with Stage 1, this optimization will be performed for both OWN and UWN. This stage is currently in progress; it began in late 2021 and will finish in early 2022.

Milestones

The MDAO strategy is under continuous development until high-fidelity optimization is complete. However, during this project period, the following milestones were achieved:

- Planned and executed the first-stage nacelle placement selection study
- Settled the formulation for the second-stage study
- Launched initial runs of the second-stage study

Major Accomplishments

- Stage 1 and 2 strategies, and potential risks, were planned and discussed with FAA technical advisors in advance.
- Our plan was implemented with a sufficient schedule margin such that we could completely redo the Stage 1 analysis upon discovering an error in our first attempt.
- We identified potential sources of uncertainty that would influence the strategy in the final, remaining period of performance in 2022.

Publications
None

Outreach Efforts
None

Awards
None

Student Involvement
- Mengzhen and Bilal Mufti are continuing PhD students who contributed by testing different MDAO formulations using coupled propulsion cycle and CFD analyses.
- Anish Vegesna, Marc Koerschner, Sam Crawford, and Andrew Burrell contributed to system/mission analysis formulation.

Plans for Next Period
The remaining six months of performance in 2022 will focus on final execution of the MDAO process and additional supporting studies using the optimization environment. In particular, we will integrate the aero-propulsion analysis with a wider system-level mission analysis.

References
Jones, D.o R., Schonlau, M., & Welch, W. J. (1998). Efficient global optimization of expensive black-box functions. Journal of Global Optimization, *13*, 455–492. https://doi.org/10.1023/A:1008306431147

Vassberg, J., Dehaan, M., Rivers, M., & Wahls, R. (2008). Development of a common research model for applied CFD validation studies [Paper presentation]. 26th AIAA Applied Aerodynamics Conference.

Task 2 - Select Aero-Propulsion Integration Method
Georgia Institute of Technology

Objective(s)
One of the most computationally intensive aspects of the MDAO formulation is the aero-propulsion coupling analysis problem. The discipline of aerodynamics uses results from propulsion cycle analysis (the Numerical Propulsion System Simulation [NPSS] code) as boundary conditions, and vice-a-versa. A valid MDA solution can be found only when these coupling variables shared between disciplines converge. There are different MDA methods to achieve such interdisciplinary closure, and they each have different costs with respect to the number of function calls.

In our study, each CFD simulation can cost at least O(1000 core-hours), so it was important to minimize the number of iterative function calls to converge a single MDA.

Research Approach
The overall MDAO design problem discussed in the previous task has constraints related to physical equilibrium. These were restated as equality constraints for interdisciplinary consistency:

- Core flow consistency: $h_1 = \left|W_7^{NPSS} - W_7^{CFD}\right| \leq \epsilon_1$
- Bypass flow consistency: $h_2 = \left|W_{17}^{NPSS} - W_{17}^{CFD}\right| \leq \epsilon_2$
- Inlet pressure recovery consistency: $h_3 = \left|\eta_{PR}^{NPSS} - \eta_{PR}^{CFD}\right| \leq \epsilon_3$
- Streamwise force balance: $h_4 = \left|\sum F_x^{CFD} + F_x^{FLOPS}\right| \leq \epsilon_4$
- Stream-normal or lift force balance: $h_5 = \left|C_L^{CFD} - C_L^{Target}\right| \leq \epsilon_5$

In these equations, W is the weight (or mass) flow, with the subscripts 7 and 17 indicating the engine stations equivalent to the CFD boundary condition plenum for exhaust flow. F_x^{FLOPS} is the streamwise force contribution from empirical drag models for components other than the wing-body-nacelle modeled in CFD. All of these constraints h_i were set to small tolerances ϵ_i.

Several MDA methods were tested with different levels of geometric complexity before selecting a final method. Initial research focused on a relatively simple, two-dimensional axisymmetric, isolated nacelle to test MDA strategies using a subset of the above constraints h_i. For example, a simple looping method (Gauss-Seidel) was used in Figure 4.

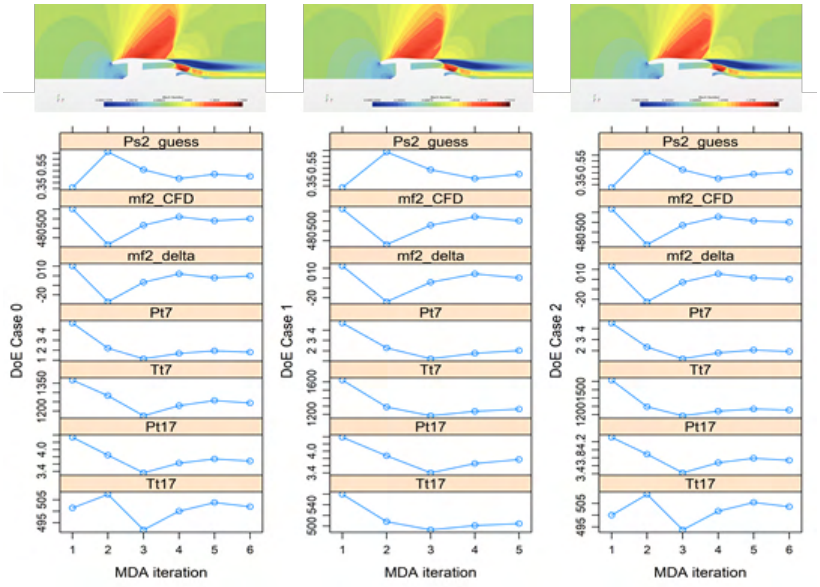

Figure 4. Example convergence history of aero-propulsion coupling variables for three design cases of a 2-D/axisymmetric nacelle.

During this research, we realized an important potential discrepancy between NPSS propulsion cycle assumptions and CFD boundary conditions. Specifically, the "0-D" NPSS code does not spatially discretize flow equations but rather connects analytically/empirically tuned flow equations for different turbomachinery elements at different stations in the engine. For example, at a nozzle station, 1D isentropic nozzle flow equations (with any tuning factors) can be used along with entry/exit areas to yield a solution coupled with all other cycle elements.

This nozzle element is of particular interest. In typical propulsion cycle analysis, it is assumed that the nozzle exhausts a flow to external boundary conditions, which are typically free-stream conditions. However, the nozzle exit flow may not actually reach free-stream conditions at the nominal outlet location and area. Figure 5 shows an example CFD case in which the bypass and core exhaust streams may not reach free-stream pressure at their respective, nominal "A_8" and "A_{18}" exit areas.

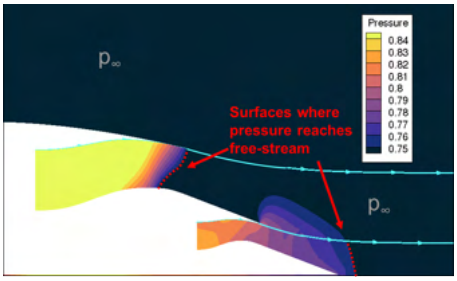

Figure 5. Areas at which exhaust streams reach free-stream pressure can be significantly different from nominal bypass and core exit areas.

This leads to a physics inconsistency between cycle analysis and CFD – which may be considered as essentially internal and external aero-thermal analyses which must pass consistent information over boundary conditions. The situation is worse in

forward-mounted OWN applications because the presence of a wing aft of the engine strongly affects exhaust flow compared to the isolated engine assumed in NPSS.

Figure 6. Mach contour plot shows the influence of the wing on exhaust streams from the engine.

One of our major developments in 2021 was adjusting the aero-propulsion MDA problem to enforce the consistency constraints. We achieved this by manipulating fictitious "exit areas" A_8 and A_{18} in the propulsion cycle analysis to help converge the MDA consistency constraints shown earlier. This is tantamount to an iterative CFD-based calibration of an NPSS model to account for complex OWN aero-propulsive interactions.

In 2021, we tested several different MDA and MDAO architectures to find a method that efficiently enforces the five MDA equality constraints listed earlier (h_1, h_2,…,h_5). For example, Figure 7 shows a snapshot of a Bayesian adaptive sampling approach based on Lee (2012) that progressively learns the settings for coupling variables that most likely satisfy the constraints.

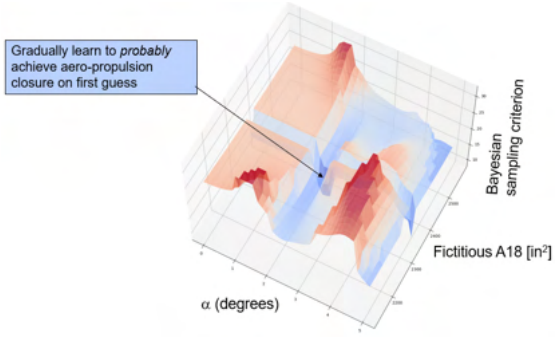

Figure 7. Bayesian method shows regions of the coupling variable domain that have a high probability of satisfying MDA closure constraints.

We ultimately selected a simple method based on the macro scripts of the commercial Star-CCM+ CFD code. This was an intrusive alteration of the CFD solution process to enforce the MDA constraints. Surrogate NPSS models were created and included inside the CFD solver script. While the CFD code iteratively solves its governing equations with respect to flow-field state variables, it also manipulates coupling variables by querying the NPSS surrogates until MDA closure is achieved.

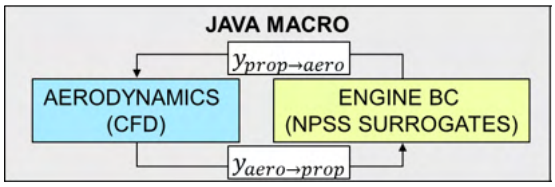

Figure 8. Final aero-propulsion coupling method relies on solver macros to intrusively enforce MDA consistency within the CFD code.

Milestone(s)

- Tested various methods for aero-propulsion coupling
- Tested direct multi-disciplinary feasible (MDF) method on 2D axisymmetric, isolated nacelles
- Tested direct multi-disciplinary feasible (MDF) method on full aircraft
- Tested rejection sampling method using 3D nacelle and wing (no fuselage)
- Tested Bayesian adaptive sampling method for 3D nacelle and wing
- Tested Fully coupled, intrusive method with full aircraft wing-body-nacelle.

Major Accomplishments

- Selected and implemented an aero-propulsion MDAO method. We specifically implemented a fully coupled method to incorporate propulsion cycle surrogate models within CFD macro solver scripts; this method is currently in use in Stage 2 optimization.

Publications

None

Outreach Efforts

None

Awards

None

Student Involvement

Bilal Mufti and Mengzhen Chen tested different MDA architectures using CFD and NPSS propulsion cycle analysis.

References

Lee, C., & Mavris, D. (2012, July). Bayesian collaborative sampling for aero-propulsion design of an engine and nacelle [Presentation]. 48th AIAA/ASME/SAE/ASEE Joint Propulsion Conference & Exhibit.

Martins, J. R. R. A., & Lambe, A. B. (2013). Multidisciplinary design optimization: A survey of architectures. AIAA Journal, *51*(9), 2049-2075.

Plans for Next Period

None

Task 3 - Create Aircraft Mission and Engine Models

Georgia Institute of Technology

Objective(s)

An aircraft-level model is necessary to compute fuel burn for a specified mission and develop a corresponding engine model for use within CFD.

Research Approach

This model wasin the Environmental Design Space (EDS) framework [1], which integrates the engine cycle analysis code NPSS, the engine weight prediction tool WATE++, and the aircraft performance and mission analysis code FLOPS. The main ingredients for an aircraft model are as follows:

1. Development of an engine architecture model in NPSS
2. Selection of engine cycle design variables
3. Development of an airframe model in FLOPS
4. Specification of requirements such as a mission profile, desired range, cruise Mach number and altitude, etc.

The baseline engine selected for this vehicle is based off a notional Pratt and Whitney geared turbofan (the PW1133GTF). A general model of the mechanical design, geometry, and thermodynamics of the engine was created in NPSS using publicly available information. This model was then 'calibrated' to International Civil Aviation Organization (ICAO) databank values of sea level static thrust and fuel flow, based on the assumption that the calibration factors applied for that flight condition are valid throughout the operating envelope. However, because the engine is rubberized, the engine can be scaled up or down in thrust for a fixed thrust to weight ratio (T/W), based on the results of the mission analysis. The baseline T/W selected for this vehicle is 0.31, based on public information for the A320neo, which is in the same passenger class considered for this study.

The airframe model in FLOPS was built around the CFD geometry of the vehicle. Key variables like fuselage length, width, depth, wing planform area, aspect ratio, taper ratio, quarter chord sweep, and dihedral were matched between the CFD geometry and the FLOPS representation of this geometry. These variables impact the weight and aerodynamic performance predictions in FLOPS. The FLOPS aircraft model is sized for 150 passengers, with an assumed weight of 225 pounds per passenger (weight of the passenger + baggage). The design range is specified to be 3415 nmi, with a cruise Mach number of 0.8 at 39,000 ft. A reserve mission for a 200 nmi trip to an alternate airport is also part of the requirements.

The mission analysis was initially conducted with FLOPS internal predictions for aerodynamics. The resulting engine dimensions and engine deck were then used to update the CFD model of the engine (both the geometry and boundary conditions). Reynolds-averaged Navier-Stokes (RANS) simulations of the airframe and engine (under-wing) were performed at cruise for an angle of attack sweep to generate a drag polar. A typical cruise part power condition is assumed to obtain the engine boundary conditions for this polar run. The resulting polar was then used to 'tune' the FLOPS internal aerodynamic predictions by adjusting FLOPS scaling factors on parasitic and induced drag (referred to as FCDO and FCDI in FLOPS terminology) such that the cruise polar predicted by FLOPS matched the polar generated by CFD. Following this tuning, EDS was re-run using the same inputs as before to determine a new engine size that meets the mission requirements. This new engine was used for all subsequent CFD analyses on both the OWN and UWN configurations.
Although EDS and CFD should theoretically be evaluated in a coupled manner until there is consistency between the engine used in the mission analysis and the engine used to generate the polars that feeds into the mission analysis, this iterative procedure is quite costly. As such, only a one-pass update was used to establish the vehicle model and the engine model in CFD. Overall, the focus of our project is to solve the aero-propulsive coupling problem within the CFD domain. Thus, for a fixed engine size, our goal was to match the engine operating conditions and inputs assumed by the NPSS model to those in the CFD domain through an iterative exchange of boundary conditions between the two disciplines, as described in the previous section. The engine size convergence between the NPSS model and that assumed in CFD is not closed. Table 1 and Figure 9 summarize some key characteristics of the airframe and engine model.

Table 1. Summary of 150-passenger aircraft model.

Name	Value
Fuselage Length (ft)	128.7
Fuselage Max Width (ft)	12.2
Fuselage Max Depth	12.2
Wing Planform Area (ft^2)	1642
Wing Aspect Ratio	8.4
Wing Quarter Chord Sweep (°)	33.76
Wing Taper Ratio	0.2
Wing Dihedral (°)	7.95
Design Payload (lb)	33,750
SLS Thrust/Engine (lb)	26,580
Thrust to Weight Ratio	0.31
Design Fan Pressure Ratio	1.525
Overall Pressure Ratio	47.91
Bypass Ratio	11.06
Design Range (nmi)	3451
Cruise Mach	0.8
Cruise Altitude (ft)	39,000

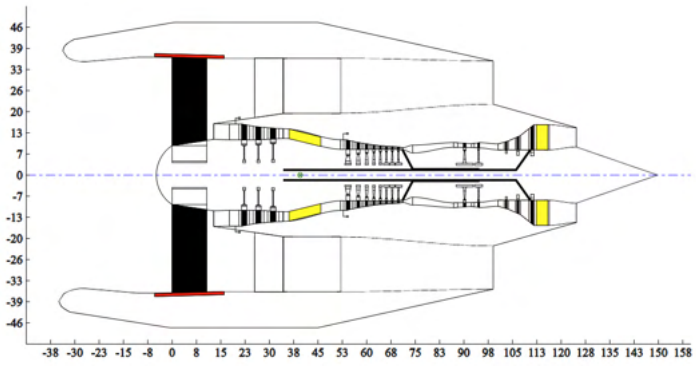

Weights		Dimensions	
Bare Engine Weight	4928.5	Engine Length	124.7
Accessories Weight	731.2	Engine Pod C.G.	39.5
Engine Weight	5659.7	Engine Max Diameter	72.6
Inlet/Nacelle Weight	89.4	Nacelle Max Diameter	0.0
Total Engine Pod Weight	5749.1	Total Engine Pod Length	124.7

Figure 9. WATE++ outputs for the final engine model used in CFD (all dimensions are in inches, and weights are in pounds).

Milestone
Completed initial system-level modeling to compute fuel burn and develop an engine model.

Major Accomplishments
Developed an engine model, in terms of geometry and boundary conditions, for use in CFD analysis of both the OWN and UWN configurations.

Publications
None

Outreach Efforts
None

Awards
None

Student Involvement
None

References
Nunez, L. S., Tai, J., & Mavris, D. N. (2021). The environmental design space: Modeling and performance updates [Presentation]. AIAA SciTech Forum. https://doi.org/10.2514/6.2021-1422.

Plans for Next Period
We will use the existing vehicle model, with our latest CFD-tuned drag polars, for mission analysis on both OWN- and UWN-optimized geometries to compare fuel burn differences.

Task 4 - Reduce Dimensionality Using Active Subspace Methods

Georgia Institute of Technology

Research Approach

The external shape of aerodynamic bodies, such as wings and nacelles, is characterized by complex and detailed surfaces. In turn, the definition of these surfaces necessitates many design parameters. The design problem in our current study contains a total of 45 variables, which are listed in Table 2. This large number of design variables hinders the exploration of the aircraft design due to a phenomenon referred to in the machine learning literature as the curse of dimensionality. To effectively tailor the airframe for a given engine location, steps must therefore be taken to reduce the dimensionality of the design space to a more reasonable value.

Table 2. List of original design variables before reduction.

Group	Variable Name	Dimension
Nacelle	Highlight lip radius	1
	Cowl maximum radius	1
	Cowl maximum radius location	1
	Cowl trailing edge angle	1
	Cowl trailing edge curvature	1
	Inlet throat location	1
	Nacelle X location	1
	Nacelle Z location	1
Wing	Wing CST coefficients (upper surface)	16
	Wing CST coefficients (lower surface)	16
	Wing twist distribution	4
Aircraft	Angle of attack	1
	Total	**45**

We reduced the dimensionality of the design space using the active subspace method described by Constantine (2015), which is a type of supervised dimensionality reduction technique. This method assumes a generic function that depends on many inputs and identifies a linear subspace of the input spaces that is responsible for most of the variability of the function. The active subspace is defined using an orthogonal basis in which the vectors represent a linear combination of the original design variables. Designs in the original space can then be projected into the active subspace, and the resulting coordinates are called the active variables. Note that the transformation, from the active variables to the original design variables, is also straightforward as it only requires the transpose of the computed orthogonal basis. Conceptually, the active subspace can alternatively be considered as a rotated set of axes in the design space that best captures the variation in the function, as shown in Figure 10.

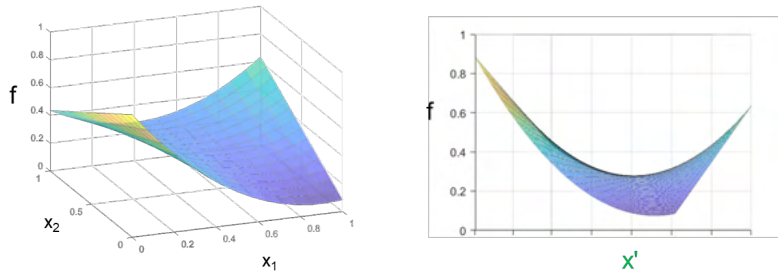

Figure 10. Notional view of the active subspace for two original design variables (left). The rotated view (right) shows that a single new variable x' captures important features of function f.

The classical active subspace method requires the computation of the gradient of the function of interest. However, in the last few years, some authors have proposed alternative methods that can extract the subspace in a gradient-free manner. One such methods is the manifold optimized active subspace (MOAS), which was initially proposed by Tripathy et al. (2016)

and improved by Rajaram et al. (2020). The MOAS method uses a Gaussian process (GP) to link the function inputs and outputs and obtains the active subspace by maximizing the likelihood of the GP via a manifold optimization algorithm. While the analysis tools used in this work can provide gradient information, the airframe uses the gradient-free MOAS approach. This decision was motivated by the additional computational cost of computing the gradient and the result of initial testing that showed noise in the gradient results, which negatively impacted the accuracy of the active subspace. The MOAS results were computed using the framework developed by Gautier et al. (2020), which is openly available[1].

Although the active subspace method can facilitate the exploration of a high-dimensional design space, it still requires generation of a substantial amount of training data. This can be quite costly when used in combination with high-fidelity RANS simulations. To further reduce the computational cost of design exploration, the active subspace in this work was computed using inviscid results obtained with Cart3D. The computed subspace was then used directly for the generation of RANS results. While the inviscid active subspace is likely different than the RANS active subspace, it is assumed that the difference between the two is relatively small because the aerodynamic performance of the aircraft is expected to depend strongly on inviscid effects such as shock waves and induced drag. The potentially lower accuracy of our approach is also compensated by the inexpensive generation of inviscid data.

Milestone(s)

Compared and selected active subspace methods for dimension reduction.

Major Accomplishments

- Active subspace variables were used successfully in the Stage 1 design study.
- Variables were selected for ongoing Stage 2 optimization.

Publications

None

Outreach Efforts

None

Awards

None

Student Involvement

Bilal Mufti and Mengzhen Chen contributed to CFD implementation and testing.

References

Constantine, P. (2015). *Active subspaces: Emerging =ildeas for dimension reduction in parameter studies.* Society for Industrial and Applied Mathematics. https://doi.org/10.1137/1.9781611973860

Gautier, R., Pandita, P., Ghosh, S., & Mavris, D. A fully bayesian gradient-free supervised dimension reduction method using gaussian processes," 2020, arXiv preprint arXiv:2008.03534

Rajaram, D., Gautier, R. H., Perron, C., Pinon-Fischer, O. J., & Mavris, D. (2020). Non-intrusive parametric reduced order models with high-dimensional inputs via gradient-free active subspace [Presntation]. AIAA AVIATION Forum. https://doi.org/10.2514/6.2020-3184

Tripathy, R., Bilionis, I., & Gonzalez, M. (2016). Gaussian processes with built-in dimensionality reduction: Applications to high-dimensional uncertainty propagation. Journal of Computational Physics, *321*, 191-223. https://doi.org/10.1016/j.jcp.2016.05.039

Plans for Next Period

The surrogate may be updated and used along with aero-propulsion optimization results for final conclusions.

[1] Source code available at https://gitlab.com/raphaelgautier/bayesian-supervised-dimension-reduction

Task 5 - CFD Grid Sensitivity Analysis

Georgia Institute of Technology

Objective(s)

The goal of this task is to generate CFD grids of different resolutions and compare the solutions for accuracy. The impact of the accuracy on the fuel burn calculations was quantified. The results were used to guide MDAO convergence criteria such that the optimization is not continued beyond the uncertainty "floor" of the physics analysis.

Research Approach

STARCCM+ Reynolds Averaged Navier Stokes CFD solver was used for this optimization study. The STARCCM+ in-built unstructured grid generator was used to generate hybrid volume mesh containing orthogonal prismatic cells (also known as prism cells) near the surface to resolve the boundary layer. and polyhedral cells were generated for the remaining volume mesh. Based on a survey of recent literature, it was found that previous OWN configuration optimization studies have used meshes ranging from 0.8M to 30M cells [1-3]. Therefore, for this study, detailed grid sensitivity analysis before finalizing the grid to establish a reference uncertainty floor. The six grids that were used (see Table 3) ranged from the coarsest size of 19.5M cells to the finest size of 475M cells, with the latter being used as the reference case for comparing the accuracy. The net L/D calculation error for all cases relative to the reference case was within 2% for the coarsest grid. Based on these findings, 76M grid was chosen for the optimization study.

Table 3. Grid convergence study results.

	CFD mesh cell count					
	19.5M	33M	76M	161M	303M	475M (Reference)
% L/D Error	1.955	1.495	0.476	-0.329	0.179	0

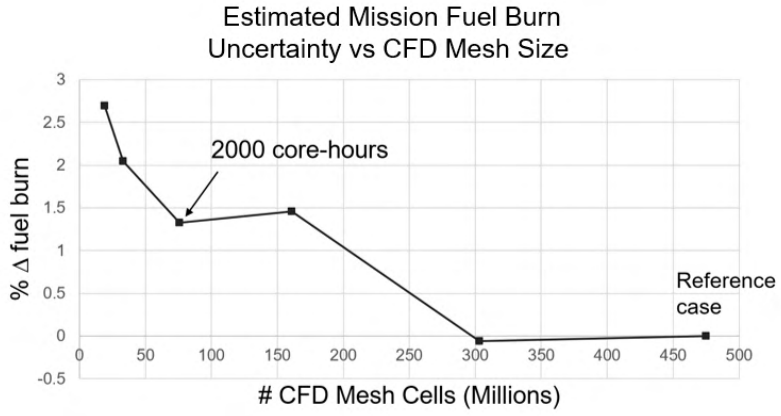

The CFD error in the drag computations associated with different grid sizes was propagated to the change in mission fuel burn via a rapid estimate. This study was performed using a modified version of FLOPS that allows user-specified data tables for the aerodynamic model of aircraft. As before, the change in the drag coefficient (ΔC_D) for only the cruise condition was obtained for all cases by keeping the drag value obtained from the 475 million cell grid as baseline. To obtain a rough estimate of the uncertainty impact of CFD mesh-related error, the ΔC_D was applied to the empirically based aerodynamics models in FLOPS. The drag polar for complete aircraft at different flight conditions was computed using empirical drag estimation techniques (EDET). This baseline drag polar was perturbed by adding ΔC_D using a blending function, such that the change in drag is maximized at the flight conditions at which ΔC_D was computed and decreases linearly as we change the Mach number.

Table 4. CFD error propagation to mission fuel burn calculations.

Grid Size (Millions)	ΔC_D	Estimated % Discrepancy in Mission Fuel Burn
19.5	6.78E-4	2.69
33	5.19E-4	2.05
76	3.37E-4	1.32
161	3.72E-4	1.46
303	-0.154E-4	-0.06
475 (Reference)	**0**	**0**

When examining the CFD solutions, there were often only subtle physical differences in flowfields. For example, there was over a 2% discrepancy in the estimated mission fuel burn between the two mesh settings shown in Figure 11. However, much of the recently published OWN literature may be qualitatively similar to the coarser of these two mesh settings.

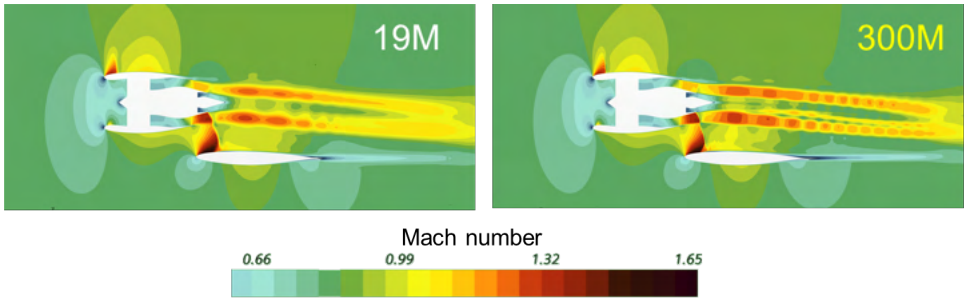

Figure 11. Subtle differences in the flowfields of different mesh cell counts result in significant discrepancies in mission fuel burn.

Milestone(s)
Completed mesh sensitivity study.

Major Accomplishments
The uncertainty impact of CFD mesh was propagated to uncertainty in the system-level metric (i.e., fuel burn).

Publications
None

Outreach Efforts
None

Awards
None

Student Involvement
PhD student Bilal Mufti propagated the CFD numerical uncertainty through the mission analysis to estimate its effect on fuel burn.

References
Berguin, A., Renganathan, S. A., Ahuja, J., Chen, M., Tai, J., & Mavris, D. N. (2018). Sensitivity analysis of aero-propulsive coupling for over-wing-nacelle concepts [Presentation]. 2018 AIAA Aerospace Sciences Meeting.

Fujino, M., & Kawamura, Y. (2003). Wave-drag characteristics of an over-the-wing nacelle business-jet configuration Journal of Aircraft, *40*(6), 1177-1184.
Hill, G. A., Kandil, O. A., & Hahn, A. S. (2009). Aerodynamic investigations of an advanced over-the-wing nacelle transport aircraft configuration. Journal of Aircraft, *46*(1), 25-35.

Task 6 - First Stage Design – Nacelle Location Selection

Georgia Institute of Technology

Objective(s)

To control the "curse of dimensionality," the MDAO process was staged into two steps. The first step focused on determining the nacelle location and was followed by more detailed shape optimization in the ongoing Stage 2 design.

Research Approach

A parametric optimization approach (formulated in Task 1) was implemented.

The efficient, integrated aero-propulsion MDA method had not yet been developed by this period of the project. Due to the expected high cost of MDA convergence for each design point, an open-loop aero-propulsion analysis was used for the first-stage study to explore nacelle locations.

Recall that a parametric optimization approach was used to minimize $f = f(\underline{\mathbf{X}}_{parameter}, \underline{\mathbf{X}}_{choice})$ with respect to shape variables $\underline{\mathbf{X}}_{choice}$ given particular settings of $\underline{\mathbf{X}}_{parameter}$. The parameter variables are the nacelle position, discretized as a 3x5 grid of engine reference location points as shown below in Figure 12.

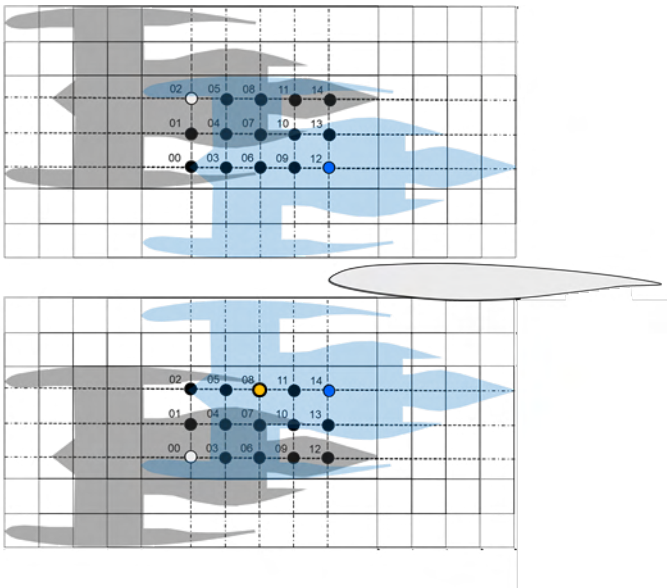

Figure 12. Grid of nacelle locations for OWN and UWN. Dots show the positions of reference locations in the engine.

The objective function is a weighted sum of L/D and excess thrust, each normalized by a reference solution in the middle of the nacelle location domain shown in Figure 12. The sign is flipped to follow the optimization convention in which lower values are better. There are two choice variables which are active subspace variables – they are hybrids or combinations of 45 wing and nacelle variables that are reduced according to the methods described in an earlier task.

A Gaussian process regression model was fit to an initial seed of warm-start design points. An expected improvement (EI) sampling criterion was calculated with respect to the current best solution for each nacelle position. The objective function is shown in Figure 13 for OWN and Figure 14 for UWN.

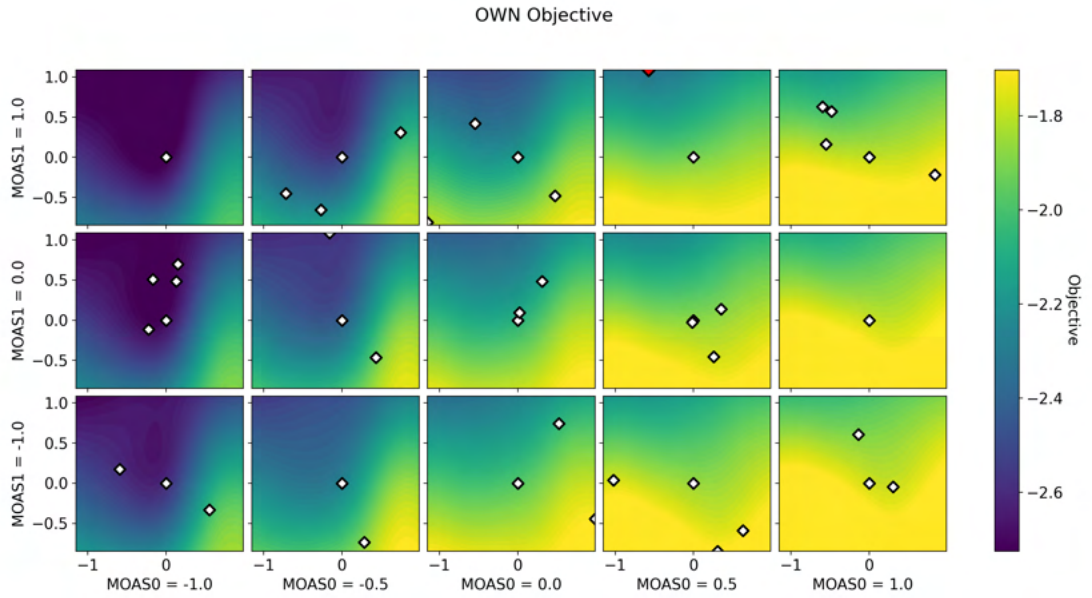

Figure 13. Parametric adaptive sample results for OWN. Lower is better. MOAS0 is nacelle x-position (streamwise) and MOAS1 is the z-position (vertical) of the nacelle. Within each box, the two axes are active subspace variables that combine nacelle and wing shape variables.

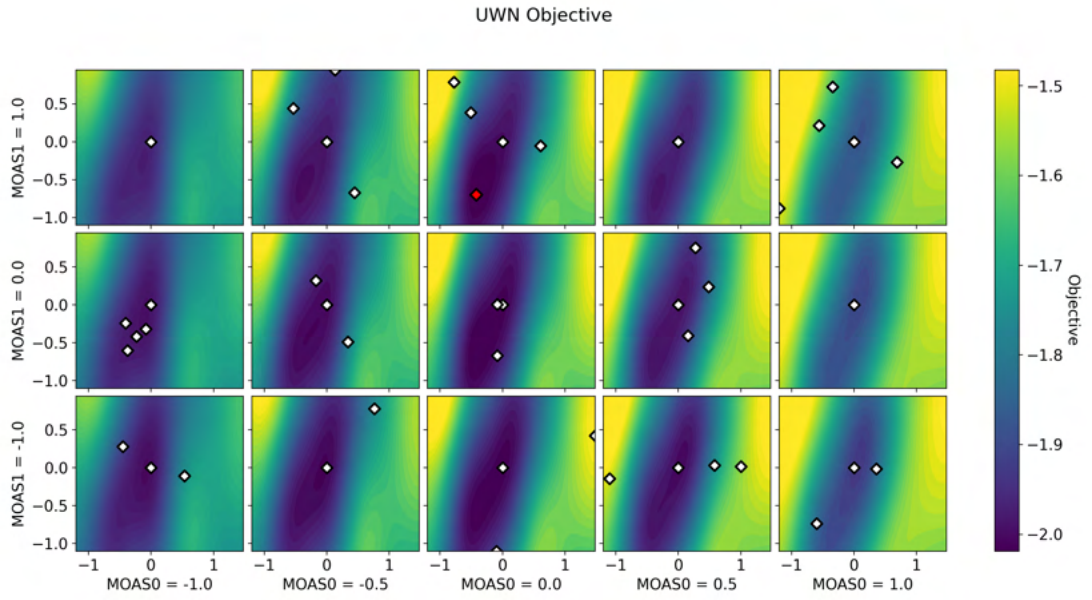

Figure 14. Parametric adaptive sample results for UWN. Axes are defined as in Figure 13.

We performed a sequential sampling process until the EI was roughly of order O(1%) of the objective function, which corresponds to the numerical uncertainty due to the CFD mesh density.

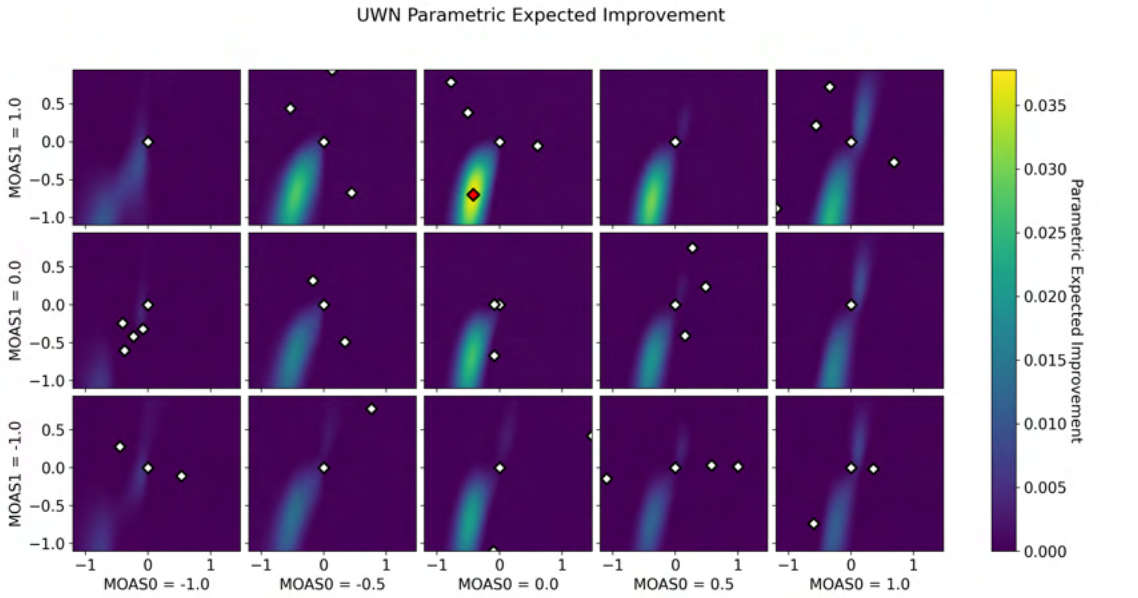

Figure 15. Example expected improvement results during the UWN adaptive sampling campaign. Note that the scale of the expected improvement is for the sum of the normalized lift-to-drag ratio and excess thrust.

The results in Figure 15 show that the problem is not sufficiently constrained, because the boxes to the top left (i.e., farther forward and higher than the wing) are clearly more favorable. There are no physics in the present MDAO scope to prevent an optimizer from continuing to move in that direction outside the specified design domain. Therefore, a subjective decision was made to a freeze single representative OWN location and pursue further wing/nacelle shape optimization. The UWN location was similarly frozen at its CRM baseline. These representative locations are shown in Figure 16.

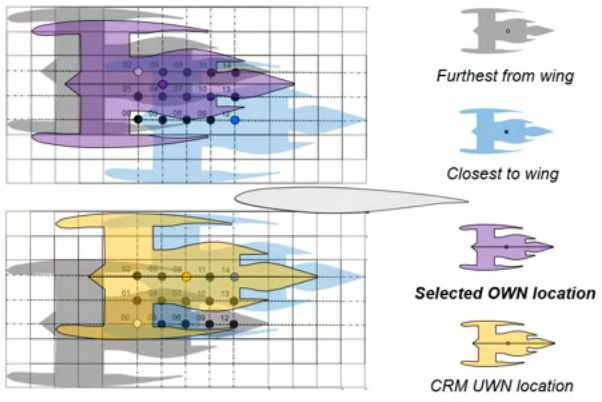

Figure 16. Subjective nacelle locations chosen for Stage 2 detailed optimization.

These decisions on nacelle locations were made in consultation with FAA advisors, with reference to our parametric optimization results. This was a human decision and therefore suffers from arbitrariness; however, this was not the result of ignorance of rigorous optimization methods, but rather an unavoidable consequence of limiting our scope to aero-propulsion physics. In future research, a detailed pylon design as well as structures and flight mechanics discipline would penalize nacelle placements that are too high or too far from the wing. For the present study, the nacelle location selections shown above will be used for deeper optimization. This will likely be followed by a sensitivity study of the Stage 2 optimum design with respect to small perturbations in nacelle x,z locations.

Milestone
Completed adaptive sampling for OWN and UWN to provide estimates of realizable optimum performance for a grid of nacelle positions.

Major Accomplishments
Selected baseline nacelle locations for OWN and UWN in discussion with FAA technical advisors

Publications
None

Outreach Efforts
None

Awards
None

Student Involvement
Bilal Mufti and Mengzhen Chen supported the CFD and study of mission fuel burn impacts

References
None

Plans for Next Period
The baseline nacelle locations selected in this task will be used in an expanded MDAO in the next stage of our analysis.

Task 7 - Create ANOPP Noise Surrogate Model
Georgia Institute of Technology

Objective(s)
The goal of this task is to use a noise analysis code, such as the ANOPP, to generate approach, cutback, sideline, and cumulative noise data via a design of experiments. This will allow surrogate models to be fit to the data set to predict changes in aircraft noise due to nacelle location.

Research Approach
ANOPP was selected as a suitable noise analysis code based on the required level of detail and the tools available. Five-level full factorial and 100-case Latin hypercube design of experiments were combined into a single experimental design to thoroughly sample the nacelle location design space within ANOPP. The ANOPP noise responses are fit to the nacelle location parameters using a single-layer artificial neural network with hyperbolic tangent nodes, resulting in a root mean square EPNdB error of less than 0.105.

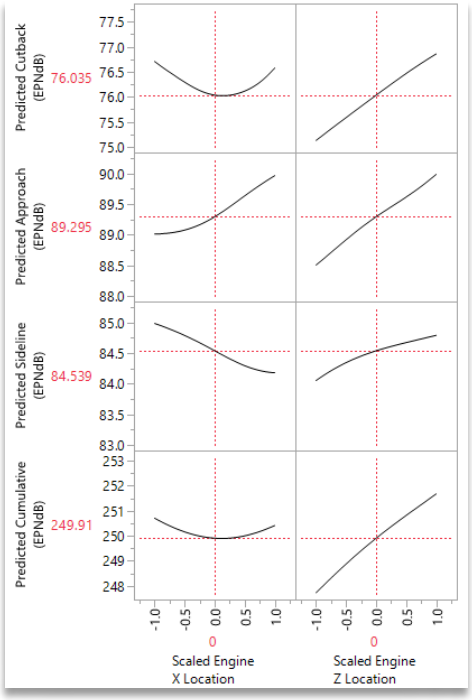

Figure 17. Example view of the Aircraft Noise Prediction Program surrogate model.

Milestone(s)
Performed initial ANOPP noise analysis.

Major Accomplishments
Artificial neural networks were fit to the approach, cutback, sideline, and cumulative forward mounted OWN and UWN noise responses as a function of the nacelle location parameters. This directly supported Task 6 (generating data to select the nacelle location).

Publications
None

Outreach Efforts
None

Awards
None

Student Involvement
Andrew Burrell ran ANOPP and fit surrogate models to the noise responses.

References
Zorumski, W. E. (1982). Aircraft noise prediction program, parts I & II (Report No. NASA TM-83199.) National Aeronautics and Space Administration.

Plans for Next Period
The surrogate may be updated and used along with aero-propulsion optimization results for final conclusions.